7-2006

The Effect of a Modified Downcomer on the Hydrodynamics in an External Loop Airlift Reactor

Samuel T. Jones
Iowa State University

Theodore J. Heindel
Iowa State University, theindel@iastate.edu

The Effect of a Modified Downcomer on the Hydrodynamics in an External Loop Airlift Reactor

Abstract

Gas holdup and superficial liquid velocity in the downcomer and riser are studied for an external loop airlift reactor with an area ratio of 1:16. Two downcomer configurations are investigated consisting of the downcomer open or closed to the atmosphere. Experiments for these two configurations are carried out over a range of superficial gas velocities from UG = 0.5 to 20 cm/s using three aeration plates with open area ratios of 0.62, 0.99 and 2.22%. These results are compared to a bubble column operated with similar operating conditions. Experimental results show that the gas holdup in the riser does not vary significantly with a change in the downcomer configuration or bubble column operation, while a considerable variation is observed in the downcomer gas holdup. Gas holdup in both the riser and downcomer are found to increase with increasing superficial gas velocity. Test results also show that the maximum gas holdup for the three aerator plates is similar, but the gas holdup trends are different. The superficial liquid velocity is found to vary considerably for the two downcomer configurations. However, for both cases the superficial liquid velocity is a function of the superficial gas velocity and/or the flow condition in the downcomer. These observed variations are independent of the aerator plate open area ratio. When the downcomer vent is open to the atmosphere, the superficial liquid velocity is initially observed to increase with increasing superficial gas velocity until the onset of choking occurs in the downcomer. Increasing the superficial gas velocity beyond the onset of choking increases the effect of choking and decreases the superficial liquid velocity. Once maximum choking is reached, the superficial liquid velocity becomes independent of the superficial gas velocity. When the downcomer vent is closed to the atmosphere, the superficial liquid velocity is initially observed to decrease with increasing superficial gas velocity as choking in the downcomer is immediately present. Once maximum choking occurs, the superficial liquid velocity once again becomes independent of the superficial gas velocity.

Keywords

external loop airlift reactor, gas holdup, hydrodynamics, liquid velocity

Comments

This is a conference proceeding from *ASME 2006 2nd Joint U.S.-European Fluids Engineering Summer Meeting Collocated With the 14th International Conference on Nuclear Engineering* 1 (2006): 1779, doi:10.1115/FEDSM2006-98011. Posted with permission.

Proceedings of FEDSM2006
2006 ASME Joint U.S. - European Fluids Engineering Summer Meeting
July 17-20, Miami, FL

FEDSM2006-98011

THE EFFECT OF A MODIFIED DOWNCOMER ON THE HYDRODYNAMICS IN AN EXTERNAL LOOP AIRLIFT REACTOR

Samuel T. Jones* **and Theodore J. Heindel**
Iowa State University
Department of Mechanical Engineering
Ames, Iowa, 50011-2161, U.S.A.
Phone: 515-294-8054, Fax: 515-294-3261
Email: sjones@iastate.edu

ABSTRACT

Gas holdup and superficial liquid velocity in the downcomer and riser are studied for an external loop airlift reactor with an area ratio of 1:16. Two downcomer configurations are investigated consisting of the downcomer open or closed to the atmosphere. Experiments for these two configurations are carried out over a range of superficial gas velocities from $U_G = 0.5$ to 20 cm/s using three aeration plates with open area ratios of 0.62, 0.99 and 2.22%. These results are compared to a bubble column operated with similar operating conditions.

Experimental results show that the gas holdup in the riser does not vary significantly with a change in the downcomer configuration or bubble column operation, while a considerable variation is observed in the downcomer gas holdup. Gas holdup in both the riser and downcomer are found to increase with increasing superficial gas velocity. Test results also show that the maximum gas holdup for the three aerator plates is similar, but the gas holdup trends are different.

The superficial liquid velocity is found to vary considerably for the two downcomer configurations. However, for both cases the superficial liquid velocity is a function of the superficial gas velocity and/or the flow condition in the downcomer. These observed variations are independent of the aerator plate open area ratio.

When the downcomer vent is open to the atmosphere, the superficial liquid velocity is initially observed to increase with increasing superficial gas velocity until the onset of choking occurs in the downcomer. Increasing the superficial gas velocity beyond the onset of choking increases the effect of choking and decreases the superficial liquid velocity. Once maximum choking is reached, the superficial liquid velocity becomes independent of the superficial gas velocity.

When the downcomer vent is closed to the atmosphere, the superficial liquid velocity is initially observed to decrease with increasing superficial gas velocity as choking in the downcomer is immediately present. Once maximum choking occurs, the superficial liquid velocity once again becomes independent of the superficial gas velocity.

Keywords: External loop airlift reactor; Gas holdup; Hydrodynamics; Liquid velocity

NOMENCLATURE

A	aerator plate open area ratio, %
A_d	downcomer open area, cm
A_r	riser open area, cm
d_c	distance between conductivity probes, cm
H	column height, m
h_d	distance between manometer taps, cm
h_m	manometer height, cm
L_d	downcomer circulation path length, m
L_r	riser circulation path length, m
P	pressure of the air-water suspension, cmH_2O
P_o	pressure of the water suspension, cmH_2O
t_p	time between tracer peaks, s
U_G	inlet superficial gas velocity, cm/s
U_{Ld}	downcomer superficial liquid velocity, cm/s
U_{Lr}	riser superficial liquid velocity, cm/s
V_d	downcomer air-water linear velocity, cm/s
V_r	riser air-water linear velocity, cm/s

* Corresponding Author

Symbols

ε_d downcomer gas holdup
ε_r riser gas holdup
ρ_G gas density, kg/m^3
ρ_L liquid density, kg/m^3

INTRODUCTION

Many bioprocessing applications use airlift reactors because of their inherent simple design, low power requirements, and ability to achieve high degrees of mixing, mass transfer, and heat transfer. Moreover, the lack of moving parts makes airlift reactors desirable for biological cultures requiring a mild, yet agitated environment [1-6].

There are two basic classifications of airlift reactors: (i) internal loop and (ii) external loop reactors [2]. An internal loop airlift reactor is basically a bubble column that has been subdivided into a riser and downcomer by the addition of a baffle or a draught tube. An external loop airlift reactor (ELALR), on the other hand, is composed of two vertical columns that have been joined together with two horizontal connectors. Thus, the distinct difference between these two groups is the presence of the horizontal connectors in the external loop airlift reactor.

An ELALR can be further subdivided into various other groups based upon the many different possible geometric configurations. Choi [3] listed three typical subcategories: (i) an ELALR with a gas-liquid separator that joins the riser and downcomer together located at the top of the reactor; (ii) an ELALR in which the downcomer is joined to the riser with two horizontal connectors at the top and bottom ends of the downcomer; and (iii) an ELALR similar to the one just mentioned with the addition of a tube above the downcomer that acts as a liquid gas separator.

Many studies involving ELALR's have indicated that reactor geometry is a key factor in determining gas holdup and liquid velocity in the downcomer and riser [3, 7-15]. When ELALR's are used as biological fermentors, liquid velocity in the riser and downcomer become key hydrodynamic factors as the circulation velocity determines if there will be dead zones in the downcomer. If the circulation velocity is too slow, dead zones will result and biological grow will cease, reducing the overall reactor productivity. Thus, prior to using an ELALR in biological applications, the effect of reactor geometry must be understood. To this end, an ELALR with varying aerator plate open area ratios and downcomer configurations will be studied and the hydrodynamic results will be presented below.

EXPERIMENTAL PROCEDURES

A schematic representation of the ELALR used in this study is shown in Fig. 1. The ELALR consists of two main parts, a 2.4 m cast acrylic riser with a 10.2 cm ID and a 2.4 m cast acrylic downcomer with a 2.5 cm ID. The downcomer and riser sections are connected with two 13.3 cm acrylic tubes with 2.5 cm ID and located at H = 5 and 127 cm, where H is the reactor height above the aerator plate. Gas is injected at the riser base through one of three stainless steel distributor plates having open area ratios A = 0.62, 0.99, and 2.22%. For each plate, 1 mm diameter holes are uniformly distributed over the

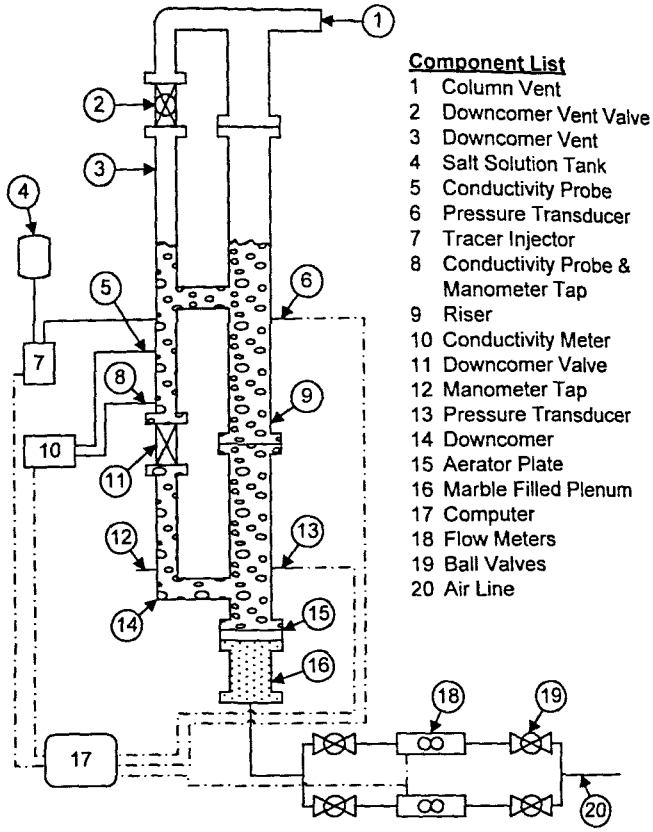

Figure 1. Experimental external loop airlift reactor schematic.

entire plate area, where the change in open area is accomplished by changing the number of uniformly distributed holes. A gas plenum is located beneath the aerator plate and filled with large gas beads (i.e., marbles) to promote uniform gas distribution into the riser.

The top of the riser and downcomer sections are joined together with a ball valve as they enter the column vent; this allows for the possibility of gas flow out of the downcomer. A gate valve is installed in the middle of the downcomer section so that when closed, the ELALR approximates a semi-batch bubble column. Two mass flow meters are used to measure the gas flow rate to cover low and high gas flow rate ranges, where the gas is filter compressed air. Two pressure transducers are installed in the riser and located at H = 10.2 and 110.5 cm. A tracer injection tap is installed in the downcomer section located at H = 108 cm. Two conductivity probes are installed in the downcomer section located at H = 63.2 and 97.8 cm. An inclined U-tube manometer is attached to the downcomer section with connections located at H = 5 and 67.13 cm. The mass flow meters, pressure transducers, and conductivity probes are interfaced to a computer controlled data acquisition system. Average inlet gas flow rate and riser section pressures are computed from measurements taken for a 2 second interval at a frequency of 1000 Hz. These measurements are taken simultaneously with every linear velocity measurement in the downcomer section.

Gas holdup in the riser section (ε_r) is measured between the two pressure transducers and is determined from the reactor

pressure drop assuming that acceleration effects are negligible [2]. Thus the total pressure drop in the reactor corresponds to the hydrostatic head; in this case,

$$\varepsilon_r = 1 - \frac{\Delta P}{\Delta P_o} \tag{1}$$

where ΔP is the difference between the average local pressure at the two pressure transducers when $U_G > 0$, and ΔP_o is the corresponding average when $U_G = 0$ (i.e., the liquid hydrostatic head).

Gas holdup in the downcomer section (ε_d) is measured using an inclined U-tube manometer, and is determined by the change in height of the water columns in the manometer, assuming acceleration effects to be negligible. For the U-tube manometer,

$$\varepsilon_d = \frac{\rho_L}{\rho_L - \rho_G}\frac{\Delta h_m}{\Delta h_d} \tag{2}$$

where ρ_L is the liquid density, ρ_G is the gas density, Δh_m is the height change of the water columns in the U-tube manometer when $U_G > 0$, and Δh_d is the distance between the manometer pressure taps on the downcomer.

The liquid linear velocity in the downcomer section (V_d) is determined using a tracer method [2, 7, 11, 16-18]. A 2 mL concentrated potassium chloride solution is instantaneously injected into the downcomer at the injector tap using an air driven injector system. The liquid conductivity response is recorded at two downstream locations using identical conductivity probes. Using the measured time interval between the conductivity peaks and the known vertical distance between the probes, the liquid linear velocity in the downcomer is determined by

$$V_d = \frac{d_e}{t_p} \tag{3}$$

where d_e is the vertical distance between the probes and t_p is the time between the conductivity peaks. The use of two identical probes eliminates the need to consider the response time of the electrodes [2, 19].

The superficial liquid velocity in the downcomer (U_{Ld}) and riser (U_{Lr}) can be calculated from the analytical relationships,

$$U_{Ld} = (1 - \varepsilon_d)V_d \tag{4}$$

$$U_{Lr} = \frac{A_d}{A_r}U_{Ld} \tag{5}$$

where A_d and A_r are the cross-sectional area of the downcomer and riser, respectively [2].

The experimental method to determine the average liquid linear velocity in the downcomer and average gas holdup in the riser for a selected superficial inlet gas velocity is as follows. Before an experiment is initiated, the tracer injector reservoir is filled with a 0.34 M potassium chloride salt solution. The ELALR is filled with tap water to a height of 142.2 cm above the aerator plate (14 column diameters). The gas is then turned on and the gas flow rate set to the desired operating point and run for ~2 minutes to ensure steady-state flow conditions. Once steady flow is achieved, data collection is initiated. Data is first collected by injecting 2 mL of the salt solution and then recording the concentration response at each conductivity probe for 10 seconds. Second, data is recorded at each of the pressure transducers and the mass flow meter for 2 seconds. Third, the liquid linear velocity in the downcomer, average gas holdup in the riser, and average superficial inlet gas velocity are calculated and recorded. Fourth, the first three steps are repeated 100 times, and then overall averages for the 100 repetitions are calculated and recorded. Note to avoid excessive liquid accumulation, 20 mL of liquid are removed after every tenth salt solution injection. Hence, the overall change in fluid height is negligible during the experiment. At the completion of the 100 injections, the ALR is drained, rinsed, and refilled with fresh water. This data collection process is replicated three times for each inlet gas velocity of interest using a randomly generated testing sequence.

The potassium chloride salt solution used as a tracer in the method just described has been shown in previous bubble column studies to significantly affect bubble coalescence and gas holdup, particularly in the transition region from homogeneous to heterogeneous flow [20, 21]. The salt concentrations evaluated in these two studies ranged from 0.005 g/cm^3 to 0.15 g/cm^3. The salt concentration in the ALR during the outlined testing procedure varies from 0 g/cm^3 initially to ~0.0004 g/cm^3 at the conclusion of each test, which is an order of magnitude smaller than those reported in the sited literature. Hence, the effect of salt concentration in the ALR on bubble coalescence and gas holdup in this case is assumed to be small.

The following experimental method is used to determine the average gas holdup in the downcomer for each selected U_G. The inclined U-tube manometer is connected to the downcomer and then the ELALR is filled with water to a height of 142.2 cm above the aerator plate (14 column diameters). The gas is turned on and the gas flow rate is set to the desired operating point and run for ~2 minutes to ensure steady state flow conditions. Once steady flow is achieved the change in manometer height is recorded. The average height change for each U_G is then converted to a gas holdup value using Eq. (2).

The above two experimental procedures are then used to determine the corresponding liquid velocity and gas holdup values for the ELALR using each of the above listed aerator plates. For each aerator plate, the ELALR is operated with the downcomer vent open and the downcomer valve open (mode OV for open vent), with the downcomer vent closed and the downcomer valve open (mode CV for closed vent), and with both the downcomer vent and valve closed (mode BC for bubble column).

Measurement uncertainties are estimated following the method provided by Figliola and Beasley [22]. The typical uncertainties associated with U_G and V_d are ±1 to 5% and ±1 to 8%, respectively, with the larger uncertainties corresponding to the lowest velocity measurements. The corresponding absolute gas holdup uncertainty is estimated to be ≈ ±0.001–0.015.

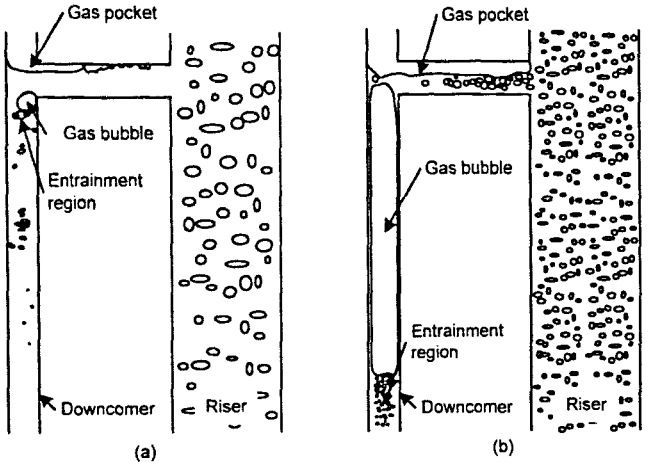

Figure 2. Gas pocket and bubble locations in the ELALR when the downcomer vent is closed (mode CV): (a) restrict flow regime ($U_G = 0.5$ cm/s) and (b) fully restricted flow regime ($U_G = 20$ cm/s).

RESULTS AND DISCUSSION

Hydrodynamic Observations

As shown in Fig. 2a, when the ELALR is operated in mode CV, a large gas pocket forms in the upper horizontal connection as soon as gas is sparged into the reactor at $U_G = 0.5$ cm/s, the lowest U_G considered. Similar results were also noted by Choi [3] for a comparable reactor. The gas pocket in the horizontal connector varies in size slightly during the experiments, but no sustained size change is observed over the range of U_G studied. After the initial formation of the gas pocket, a gas bubble forms just below the horizontal connector in the downcomer as U_G increases. This gas bubble, when present, is located between the horizontal connector and the entrainment region. As U_G increases, the gas bubble diameter begins to grow until it is nearly equal to the ID of the downcomer. Once the gas bubble diameter ceases to grow, the gas bubble length then increases as U_G increases to $U_G = 20$ cm/s (Fig. 2b).

Visual observations indicate that the liquid below the gas pocket is free of entrained gas as it enters the downcomer over the entire U_G range, indicating that gas separation occurs as the gas-liquid mixture moves through the horizontal connector, similar trends were reported in work done by others [14, 23]. In the entrainment region below the gas bubble, surface aeration is noted, and is observed to increase as U_G increases. The surface aeration at this location causes some of the gas in the gas bubble to be entrained into the liquid; however, the degree of gas entrainment is small. Most of the small bubbles entrained at this point stay close to the entrainment region while some of the small bubbles are carried about a third of the way down the downcomer. At $U_G \leq 3.5$ cm/s, very few, if any gas bubbles are present in the downcomer. When $U_G \geq 3.5$ cm/s, the number and size of small bubbles in the downcomer does increase; although, the average gas holdup in the downcomer is not measurable for any U_G studied.

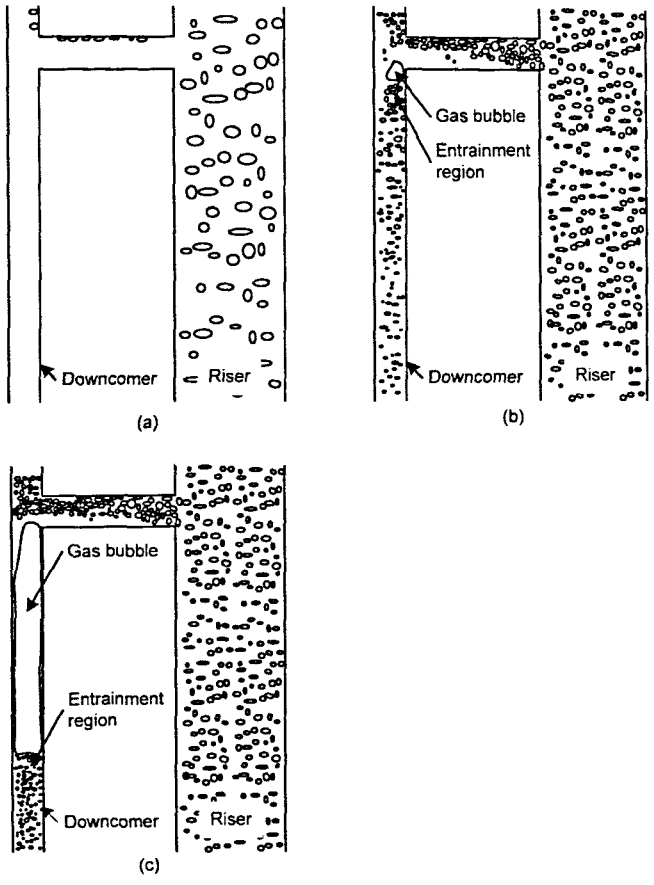

Figure 3. Gas bubble location in the ELALR when the downcomer vent is open (mode OV): (a) unrestricted flow regime ($U_G = 0.5$ cm/s), (b) restricted flow regime ($U_G = 3.5$ cm/s), and (c) fully restricted flow regime ($U_G = 20$ cm/s).

When the ELALR is operated in mode OV, the formation of the gas pocket in the horizontal connection is not observed, however, as shown in Fig. 3, a similar gas bubble does form in the downcomer. Gas bubble formation in the downcomer begins to occur at $U_G \approx 3.5$ cm/s when the fluid begins to separate from the downcomer wall due to an increase in the fluid velocity around the elbow in the upper portion of the downcomer (Fig. 3b). The gas bubble diameter and length increase as U_G increases for $3.5 \text{ cm/s} \leq U_G \leq 10$ cm/s. For $U_G \geq 10$ cm/s the gas bubble size rapidly oscillates with a mean size that appears to be independent of U_G (Fig. 3c). The cause of this rapid oscillation in size is thought to be due to the rate of gas entrainment below the gas bubble and the random escape of gas up the downcomer.

Gas entrainment in the downcomer for mode OV is initially nonexistent, as most of the gas phase that enters the horizontal connector rises to the top of the connector and then exits up the downcomer, thus the horizontal connector is acting as a phase separator. As U_G increases, the degree of separation decreases and part of the gas is pulled down into the downcomer as the liquid momentum increases. Most of the gas

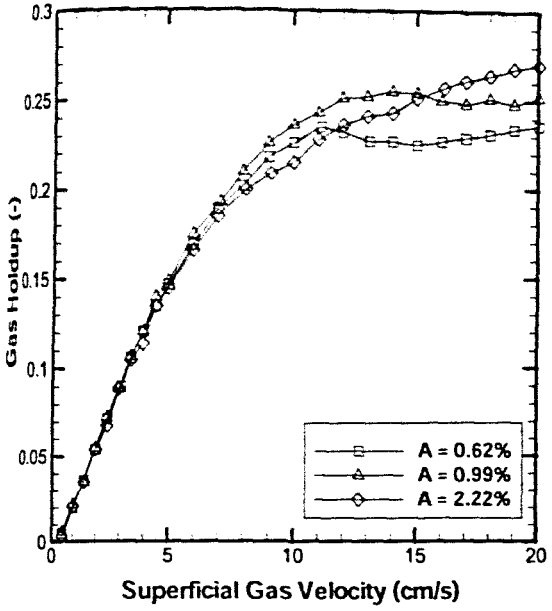

Figure 4. Gas holdup using different aeration plates when the ELALR is operated in mode BC.

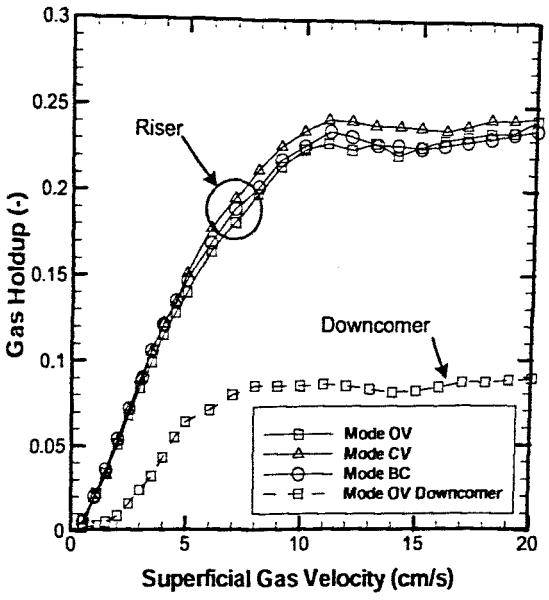

Figure 5. Effect of ELALR operation mode on gas holdup for A = 0.62%.

pulled into the downcomer separates from the liquid phase as it moves around the gas bubble (when it exists). The gas pulled into the downcomer is then re-entrained into the liquid phase in the entrainment region just below the gas bubble (Fig. 3c).

Gas Holdup

The effect of aeration plate open area on gas holdup is shown in Fig. 4 when the ELALR is operated as a bubble column (mode BC). It is observed that the open area has a negligible effect on gas holdup at low U_G, where the corresponding bubble column flow regime is homogeneous. At medium U_G, where the bubble column flow is in the transition regime, gas holdup behavior is found to deviate among the three plates. In the transition regime, when A < 1%, the gas holdup increases with increasing gas flow until a local maxima is achieved, then decreases slightly, and then begins to converge as U_G continues to increase into the heterogeneous flow regime. In the case when A = 2.22%, the gas holdup trend deviates from that with A < 1% in the transition and heterogeneous flow regimes and continually increases with increasing U_G. Similar trends have also been reported for a 15.2 cm ID semi-batch bubble column using similar aerator plates [24].

To further study the effect of U_G on gas holdup in the ELALR, the reactor is operated in modes OV and CV and compared to mode BC. The effect of ELALR operational mode on gas holdup is shown in Fig. 5 for A = 0.62%. When $U_G \leq 3.5$ cm/s, the operational mode has a negligible effect on ε_r (symbols connected by a solid line in Fig. 5). When 3.5 cm/s $\leq U_G \leq$ 10 cm/s, there appears to be slight differences in ε_r, but this variation is small, and in some cases, the degree of variation is not more than the expected measurement error. When $U_G \geq 10$ cm/s, ε_r is again independent of operational mode. It is apparent that aside from minor variations in magnitude, ε_r is, at most, a weak function of ELALR operational mode for the reactor geometry considered in this study. Similar results are observed for A = 0.99 and 2.22%.

Note that ε_d is only shown for mode OV in Fig. 5 because ε_d is negligible when the ELALR is operated in mode CV and nonexistent for mode BC. For $U_G < 2$ cm/s, $\varepsilon_d \approx 0$, which agrees with visual observations made at these operating conditions. When 3.5 cm/s $\leq U_G \leq$ 10 cm/s, ε_d increases sharply with increasing U_G. Further increases in U_G result in no change in ε_d. Note that for most cases, ε_d is approximately three times smaller than ε_r for mode OV and $\varepsilon_d \approx 0$ for mode CV.

Figure 6 shows the effect of aeration plate open area on gas holdup for mode OV operation. The ε_r trends between

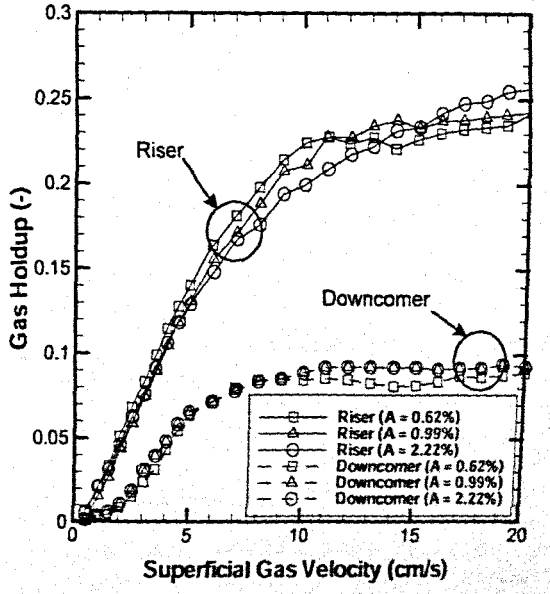

Figure 6. Aerator plate open area ratio effect on gas holdup for mode OV ELALR operation.

aeration plates for the open vent mode are similar to the variations observed when the ELALR is operated in mode BC. Figure 6 also shows no significant variation ε_d for the different aeration plates used in this study.

Liquid Circulation

The bulk density difference of the two vertical columns in an ELALR provides the driving force for liquid circulation (i.e., U_{Lr} and U_{Ld}). At steady state conditions, the driving force is balanced by reactor flow losses due to fluid friction and changes in reactor geometry [2, 19, 23, 25, 26]. Thus, as the difference between ε_r and ε_d increases with increasing U_G, the driving force must also increase due to bulk density changes associated with changing gas holdup, creating a potential for U_{Lr} to increase. However in practice, U_{Lr} may increase or decrease with U_G depending on how the reactor flow losses change with U_G. Hence, U_{Lr} can be considered to be largely a function of U_G and reactor geometry.

The effect of U_G on U_{Lr}, as a function of aerator plate open area ratio and mode of operation, is shown in Fig. 7. The aerator plate open area ratio has a minimal effect on U_{Lr} for both modes of operation. When the ELALR is operated in mode OV, U_{Lr} increases to a local maximum and then decreases sharply as U_G increases, and eventually becomes independent of U_G. Therefore, three liquid flow regimes are identified for mode OV operation: (i) unrestricted flow, (ii) restricted flow, and (iii) fully restricted flow.

In the unrestricted flow regime, U_{Lr} increases sharply with increasing U_G. This initial increase in U_{Lr} corresponds to the rapid rise in ε_r and a much smaller rise in ε_d (Fig. 6). Hence, when $U_G \leq 3.5$ cm/s, U_{Lr} is primarily a function the bulk density difference; this observation agrees with the experimental results presented by others [9, 11, 12, 23, 27].

When the bulk density difference (ε_r - ε_d) is plotted as a function of U_{Lr} (Fig. 8), the relationship between the driving force and liquid circulation becomes very evident. As a result,

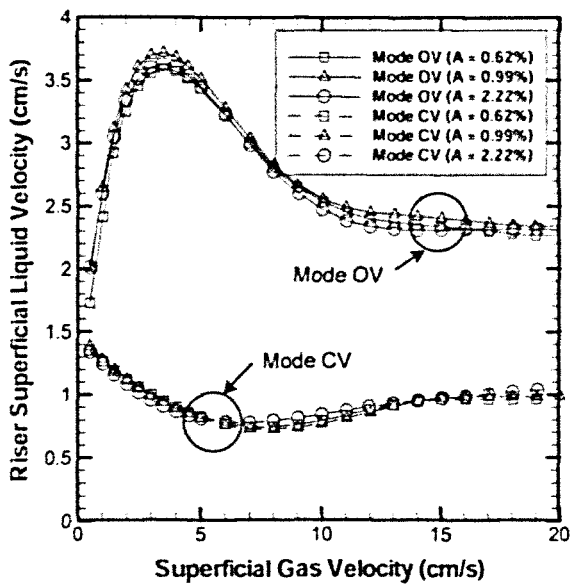

Figure 7. Aerator plate open area ratio and mode of operation effects on U_{Lr}.

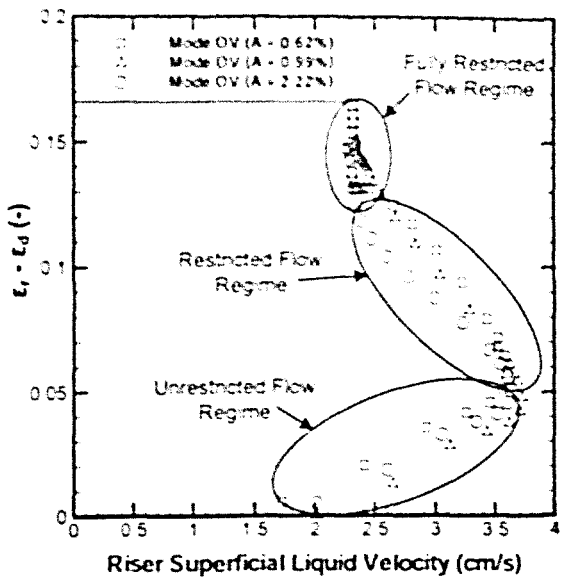

Figure 8. Relationship between driving force ($\varepsilon_r - \varepsilon_d$) and U_{Lr} as a function of aerator plate open area ratio for mode OV ELALR operation.

Fig. 8 is very useful in identifying the liquid flow regimes and their transition points. Figure 8 shows that the shift from the unrestricted flow regime to the restricted flow regime occurs at $U_{Lr} \approx 3.7$ cm/s, which roughly corresponds to the point where bubble formation is observed in the downcomer. As noted earlier, bubble formation in the top of the downcomer begins at $U_G \approx 3.5$ cm/s.

Increasing U_G in the restricted flow regime results in a decrease in U_{Lr}. Figure 8 also shows that U_{Lr} decreases in this regime as the bulk density difference increases, which is contrary to the observation made for the unrestricted flow regime. Hence, with U_{Lr} a function of the flow losses, geometry, and driving force, the flow losses are considered to dominate in this flow regime. The dominance of the flow losses in this regime is attributed gas bubble growth in the downcomer, which causes the flow losses to increase rapidly with increasing in U_G. Initially as the gas bubble begins to grow ($3.5 \text{ cm/s} \leq U_G \leq 5$ cm/s), the effective A_d to A_r ratio decreases creating a choked flow condition in the downcomer that results in the U_{Lr} local maximum shown in Fig. 7. Once the gas bubble encompasses the majority of the downcomer diameter, the gas bubble length increases for $5 \text{ cm/s} \leq U_G \leq 10$ cm/s. Gas bubble growth in this regime is a result of the bulk density difference increase and the initial flow restriction in the downcomer due to liquid separation from the downcomer wall. Hence, the driving force increases and flow losses increase faster as U_G increases in this regime causing U_{Lr} to decrease. Essentially, the downcomer flow is becoming choked.

As shown in Fig. 7, U_{Lr} continues to decrease with increasing U_G due to gas bubble development and growth until a maximum gas bubble size is reached. This transition is easily identified in Fig. 8 and occurs when the driving force becomes

independent of U_{Lr} ($\approx$ 2.4 cm/s), which corresponds to roughly U_G = 10 cm/s. Under these conditions, the liquid flow in the downcomer is fully choked and the ELALR hydrodynamics are similar to those of a bubble column.

When the ELALR is operated in mode CV, the U_{Lr} response to U_G is limited to the later two flow regimes discussed for mode OV operation (Fig. 9). As discussed in the hydrodynamics observations, a gas pocket immediately begins to form in the horizontal connection for the lowest U_G and a gas bubble forms in the downcomer soon after as U_G is increased, causing the ELALR to operate in the restricted flow regime. It is worth noting that even though ε_d exists for this mode of operation, the magnitude is so small that it can not be measured with any degree of accuracy, and thus is considered negligible. The driving force for mode CV operation becomes solely a function of ε_r, unlike mode OV where the driving force is a function of the difference between ε_r and ε_d.

For mode CV operation shown in Fig. 9, the restricted flow regime is separated into a decreasing and increasing restricted flow regime. Initially, as U_G increases, the column flow is characterized as decreasing restricted flow where, as shown in Fig. 7, U_{Lr} decreases with increasing U_G. This decrease in U_{Lr} continues until a local minimum is reached at $U_G \approx 7$ cm/s, which corresponds to $\varepsilon_r \approx 0.18$ (Fig. 5). The decrease in U_{Lr} in this regime is again attributed to development and growth of the gas bubble in the downcomer. Once the minimum U_{Lr} is reached, U_{Lr} begins to increase with increasing U_G, switching the flow regime to the increasing restricted flow regime. In this flow regime, U_{Lr} continues to increase with U_G and ε_r until $U_G \approx 14$ cm/s and $\varepsilon_r \approx 0.24$. It is important to note that the gas bubble growth is observed to be relatively constant as U_G increases throughout both restricted flow regimes, indicating that for the decreasing restricted flow regime, flow losses initially exceed the increase in the driving force. This effect then reverses as the flow regime changes to increasing restricted flow, indicating that in this regime, the driving force is larger than the flow losses.

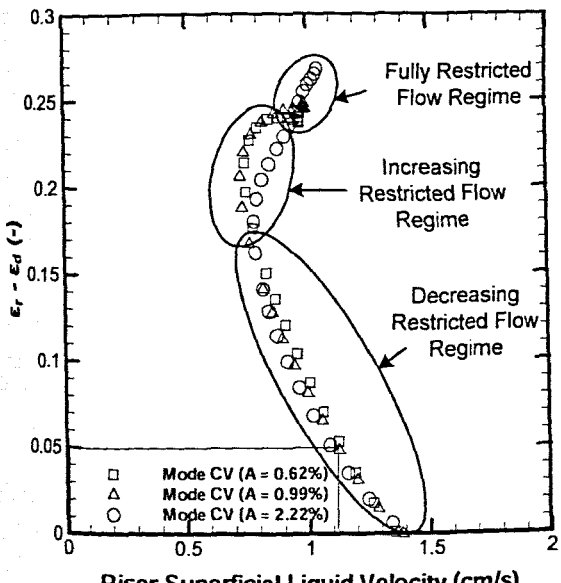

Figure 9. Relationship between driving force ($\varepsilon_r - \varepsilon_d$) and U_{Lr} as a function of aerator plate open area ratio for mode CV ELALR operation.

As shown in Fig. 7, U_{Lr} is independent of aerator plate open area ratio; however, the onset of the fully restricted flow regime for mode CV is influenced by the aerator plate open area ratio. The shift from the increasing restricted flow regime to the fully restricted flow regime occurs at $U_G \approx 13$ cm/s for A < 1%. For A = 2.22%, the transition into the fully restricted flow regime appears to occur at $U_G \approx 19$ cm/s, but more data at $U_G > 20$ cm/s is needed to fully understand the transition location for mode CV operation when A = 2.22%. As discussed for the open vent mode of operation, U_{Lr} in the fully restricted flow regime is observed to be independent of U_G.

CONCLUSIONS

Gas holdup and liquid superficial velocity results were presented for an external loop airlift reactor with three modes of operation (open downcomer vent, closed downcomer vent, and bubble column modes) for a range of aerator plate open areas ratios (A = 0.62, 0.99, and 2.22%) and superficial gas velocities ($U_G \leq 20$ cm/s). Geometry changes due to flow restrictions and mode of operation significantly affected the fluid flow hydrodynamics in the ELALR. Riser gas holdup was observed to be independent of aerator plate open area ratio and mode of operation. Downcomer gas holdup was only significant when the ELALR was operated with the downcomer vent open (mode OV). Three liquid flow regimes were identified for the riser superficial liquid velocity: (i) unrestricted flow, (ii) restricted flow, and (iii) fully restricted flow regimes. For open and closed vent downcomer operation (mode OV and CV), riser superficial liquid velocity was independent of aerator plate open area ratio, and strongly dependent on the mode of operation. For open and closed downcomer vent operation (mode OV and mode CV), riser superficial liquid velocity was a function of superficial gas velocity in the unrestricted and restricted flow regimes, and independent of superficial gas velocity in the fully restricted flow regime.

ACKNOWLEDGMENTS

This material is based upon work supported by the Natural Resources Conservation Service, U.S. Department of Agriculture, under Agreement No. NRCS 68-3475-3-151. Any opinions, findings, conclusions, or recommendations expressed herein are those of the authors and do not necessarily reflect the views of the USDA.

REFERENCES

[1] Bentifraouine, C., Xuereb, C., and Riba, J.-P., 1997, "Effect of Gas Liquid Separator and Liquid Height on the Global Hydrodynamic Parameters of an External Loop Airlift Contactor," Chemical Engineering Journal, **66**, pp. 91-95.

[2] Chisti, M.Y., 1989, "Airlift Bioreactors," Elsevier Applied Biotechnology Series, Elsevier Applied Science, London.

[3] Choi, K.H., 2001, "Hydrodynamic and Mass Transfer Characteristics of External-Loop Airlift Reactors without an Extension Tube above the Downcomer," Korean Journal of Chemical Engineering, **18**(2), pp. 240-246.
[4] Gavrilescu, M., and Tudose, R.Z., 1997, "Mixing Studies in External-Loop Airlift Reactors," Chemical Engineering Journal, **66**, pp. 97-104.
[5] Merchuk, J.C., and Siegal, M.H., 1988, "Air-Lift Reactors in Chemical and Biological Technology," Journal of Chemical Technology and Biotechnology, **41**, pp. 105-120.
[6] Snape, J.B., Zahradnik, J., Fialova, M., and Thomas, N.M., 1995, "Liquid-Phase Properties and Sparger Design Effects in an External-Loop Airlift Reactor," Chemical Engineering Science, **50**(20), pp. 3175-3186.
[7] Bello, R., Ade, Robinson, C.W., and Moo-Young, M., 1984, "Liquid Circulation and Mixing Characteristics of Airlift Contactors," The Canadian Journal of Chemical Engineering, **62**(October), pp. 573-577.
[8] Bentifraouine, C., Xuereb, C., and Riba, J.-P., 1997, "An Experimental Study of the Hydrodynamic Characteristics of External Loop Airlift Contactors," Journal of Chemical Technology and Biotechnology, **69**, pp. 345-349.
[9] Chisti, M.Y., and Moo-Young, M., 1987, "Airlift Reactors: Characteristics, Applications, and Design Considerations," Chemical Engineering Communication, **60**, pp. 195-242.
[10] Gavrilescu, M., and Tudose, R.Z., 1996, "Effects of Downcomer-to-Riser Cross Sectional Area Ratio on Operation Behavior of External-Loop Airlift Bioreactors," Bioprocess Engineering, **15**, pp. 77-85.
[11] Gavrilescu, M., and Tudose, R.Z., 1995, "Study of the Liquid Circulation Velocity in External-Loop Airlift Bioreactors," Bioprocess Engineering, **14**, pp. 33-39.
[12] Mercer, D.G., 1981, "Flow Characteristics of Pilot-Scale Airlift Fermentor," Biotechnology and Bioengineering, **23**, pp. 2421-2432.
[13] Merchuk, J.C., and Stein, Y., 1981, "Local Hold-up and Liquid Velocity in Air-Lift Reactors," AIChE Journal, **27**(3), pp. 377-388.
[14] Siegal, M.H., and Merchuk, J.C., 1988, "Mass Transfer in Rectangular Air-Lift Reactor: Effects of Geometry and Gas Recirculation," Biotechnology and Bioengineering, **32**, pp. 1128-1137.
[15] Siegal, M.H., Merchuk, J.C., and Schugerl, K., 1986, "Air-Lift Reactor Analysis: Interrelationships between Riser, Downcomer, and Gas-Liquid Separator Behavior, Including Gas Recirculation Effects," AIChE Journal, **32**(10), pp. 1585-1596.
[16] Fields, P.R., and Slater, N.K.H., 1983, "Tracer Dispersion in a Laboratory Air-Lift Reactor," Chemical Engineering Science, **38**(4), pp. 647-653.
[17] Van't Riet, K., and Tramper, J., 1991, "Basic Bioreactor Design," Marcel Dekker, Inc, New York, New York.
[18] Shah, Y.T., Stiegel, G.J., and Sharma, M.M., 1978, "Backmixing in Gas-Liquid Reactors," AIChE Journal, **24**(3), pp. 369-400.
[19] Bakker, W.A.M., Tramper, J., and Gooijer, C.D., 1993, "Hydrodynamics, Mixing, and Oxygen Transfer in the Multiple Air-Lift Loop Reactor," 3rd International Conference on Bioreactor & Bioprocess Fluid Dynamics, Cambridge, UK: Mechanical Engineering Publications Limited, pp. 49-60.
[20] Jamialahmadi, M., and Muller-Steinhagen, H., 1990, "Effect of Electrolyte Concentration on Bubble Size and Gas Hold-up in Bubble Columns," Chemical Engineering Research & Design, **68**(2), pp. 202-204.
[21] Zahradnik, J., Fialova, M., Kastanek, F., Green, K.D., and Thomas, N.H., 1995, "The Effect of Electrolytes on Bubble Coalescence and Gas Holdup in Bubble Column Reactors," Chemical Engineering Research & Design, Transactions of the Institute of Chemical Engineers, Part A, **73**(A3), pp. 341-346.
[22] Figliola, R.S., and Beasley, D.E., 2000, "Theory and Design for Mechanical Measurement," 3rd ed, John Wiley & Sons Inc, New York.
[23] Choi, K.H., and Lee, W.K., 1993, "Circulation Liquid Velocity, Gas Holdup and Volumetric Oxygen Transfer Coefficient in External-Loop Airlift Reactors," Journal of Chemical Technology and Biotechnology, **56**, pp. 51-58.
[24] Su, X., and Heindel, T.J., 2005, "Effect of Perforated Plate Open Area on Gas Holdup in Rayon Fiber Suspensions," Journal of Fluids Engineering, **127**(4), pp. 816-823.
[25] Chisti, M.Y., Halard, B., and Moo-Young, M., 1988, "Liquid Circulation in Airlift Reactors," Chemical Engineering Science, **43**(3), pp. 451.
[26] Felice, R.D., 2005, "Liquid Circulation Rates in Two- and Three-Phase External Airlift Reactors," Chemical Engineering Journal, **109**, pp. 49-55.
[27] Bello, R., Ade, Robinson, C.W., and Moo-Young, M., 1985, "Gas Holdup and Overall Volumetric Oxygen Transfer Coefficient in Airlift Contactors," Biotechnology and Bioengineering, **27**, pp. 369-381.